Water Increases the Fluidity of Intercellular Membranes of Stratum Corneum: Correlation with Water Permeability, Elastic, and Electrical Resistance Properties

Antonio Alonso,* Nilce C. Meirelles,† Victor E. Yushmanov,‡§ and Marcel Tabak‡

*Departamento de Eletrônica Quântica, Instituto de Física, †Instituto de Biologia, Universidade de Campinas, Campinas 13083–970, SP, Brazil; and ‡Instituto de Química, Universidade de São Paulo, São Carlos 13560–970, SP, Brazil

We used the spin label electron spin resonance technique to monitor the hydration effect on the molecular dynamics of lipids at C-5, C-12, and C-16 positions of the alkyl chain. Increase in water content of neonatal rat SC leads to an increase in membrane fluidity, especially in the region near the membrane-water interface. The effect is less pronounced deeper inside the hydrophobic core. The reorientational correlation time at the C-16 position of hydrocarbon chains showed a higher change up to ~18% (w/w) of water content. This behavior was accompanied by an exponential decay both in elastic modulus and electrical resistance with water content. On the contrary, the segmental motion at C-5 and C-12 positions of the chain and the permeability constant increased in the range of around 18% (w/w) up to the fully hydrated condition (58 ± 7%). Our results give a better characterization of the fluidity of SC and show that it is the principal parameter involved in the mechanism of the permeability of different compounds through skin. ***Key words: stratum corneum/ESR/hydration effect/membrane fluidity/permeability/elasticity/electrical resistance. J Invest Dermatol 106:1058–1063, 1996***

The uppermost skin layer, stratum corneum (SC), plays an important role as a low permeability membrane that reduces effectively the body water loss as well as limits the penetration of external substances into the organism. This minimal permeability to water and other solutes in both directions is assured by the intercellular lipids that form broad multilayer sheets in spaces between the corneocytes (Elias, 1975, 1983; Swartzendruber *et al*, 1989). These lipids, corresponding to about 14% of the dry weight of SC, consist of ceramides (40–50%), free fatty acids (15–25%), cholesterol (20–25%), and cholesterol sulfate (5–10%) (Gray *et al*, 1982; Long *et al*, 1985; Swartzendruber *et al*, 1987).

El-Shime and Princen (1978) and Blank *et al* (1984) have shown that the diffusion constant for water in SC increases with tissue water content. Other investigators have suggested that water is a very effective penetration enhancer for drug delivery (Barry, 1987; Potts and Francoeur, 1991). It is not clear, however, how water reduces the barrier resistance of the SC to the permeation of molecules. It is well known that an increase in lipid fluidity of both biological and artificial membranes produces an increase in its permeability (for a review see Fettyplace and Haydon, 1980), suggesting a correlation between transdermal flux and lipid fluidity (Knutson *et al*, 1986; Golden *et al*, 1987). In addition, Hadgraft *et al* (1992) have shown that topical drug permeation is affected by the structural arrangement and composition of the SC lipids. Despite this knowledge, the dynamic properties of intercellular membranes of SC are not completely characterized, and the effect of hydration on the fluidity of these membranes has not been studied in detail.

The hydration level of the SC seems to affect all of its properties, modifying even the SC affinity for water itself (Hansen and Yelin, 1972). It is well known that water causes a great increase in the elasticity of SC and that the hydrated SC is much more extensible than SC at low water content (Maes *et al*, 1983; Cooper *et al*, 1985). Changes in electrical properties of the SC as a function of the hydration level (Leveque and Rigal, 1983; Serban *et al*, 1983) have been also observed. Due to the high sensitivity, the measurements of impedance or resistance (in the case of direct current) have been widely used to evaluate the hydration of the SC (for a review see Leveque and Rigal, 1983).

In the current work, we have used the electron spin resonance (ESR) technique and the spin labels 5-, 12-, and 16-doxylstearic acids (5-, 12-, and 16-SASL, respectively) to evaluate the depth-dependent fluidity of the intercellular membranes in intact SC of neonatal rat at different hydration states. In order to gain a better understanding of the mechanisms of water-induced changes in the barrier function of the SC and also in its elasticity and electrical resistance, we have measured a hydration dependence of these parameters in neonatal rat SC.

Manuscript received September 14, 1995; revised December 21, 1995; accepted for publication January 10, 1996.

§ Permanent address: Institute of Chemical Physics, Russian Academy of Sciences, Moscow.

Reprint requests to: Antonio Alonso, Departamento de Eletrônica Quântica, Instituto de Física, Universidade de Campinas, Campinas 13083-970, SP, Brazil.

Abbreviations: ESR, electron spin resonance; SC, stratum corneum; 5-SASL, 5-doxylstearic acid spin label; 12-SASL, 12-doxylstearic acid spin label; 16-SASL, 16-doxylstearic acid spin label; WCSC, water content of stratum corneum; RH, relative humidity; WFSC, water flux in stratum corneum; EMSC, elastic modulus of stratum corneum; RTSC, rupture tension of stratum corneum; ESC, elongation of stratum corneum, and ERSC, electrical resitance of stratum corneum.

MATERIALS AND METHODS

Stratum Corneum Membranes SC was obtained from newborn Wistar rats aged less than 24 h. After sacrifice, the skin was excised and fat was removed through the use of gaze friction in distilled water. Skin was allowed to stand for 5 min in a desiccator containing 0.5 liter of anhydrous ammonium hydroxide. It was then placed floating in water, with the epidermis side in contact with water, and after 2 h the SC was removed over a filter paper and transferred to a Teflon-coated screen, extensively washed with distilled water, and allowed to dry at ambient conditions. This procedure reduced the effect of remaining epidermal tissues to a minimum. The membranes were stocked until the use in a desiccator containing a silica gel under a moderate vacuum.

Water Content of SC (WCSC) The SC was kept at 31°C in a desiccator where the relative humidity (RH) was controlled by placing 1 liter of different aqueous salt solutions. The RH levels used were: 100% RH (distilled water), 93% RH (1.4 M K_2CO_3), 81% RH (3.0 M K_2CO_3), 78% RH (saturated $CaCl_2$), 62% RH (4.7 M K_2CO_3), and 46% RH (5.7 M K_2CO_3). The samples were weighed after equilibration (3 days), and the solutions in the desiccator were replaced by 1 kg of silica gel (0% RH) in order to obtain the dry weight of SC. From such gravimetric measurements we obtained the percentage of water absorbed per total weight of SC.

Spin Labeling of SC Membranes The fatty acid spin labels 5-, 12-, and 16-SASL were purchased from Aldrich Chem Co. (Milwaukee, WI). These spin labels are stearic acid analogs, and each has a nitroxide radical fragment at the 5th, 12th, and 16th carbon positions of acyl chain, respectively. A small aliquot of stock label solution in ethanol (5 mg/ml) was put in a glass tube, and the solvent was evaporated under nitrogen gas flux. The SC sample was suspended with 200 μl of phosphate-buffered saline, pH 7.4, in the same tube. The sample consisted of about 10 mg of SC (dry weight) from a single animal cut and ground in very small pieces (final concentration, ≈50 mg/ml). The concentration of spin label was estimated as 0.5 mM. After labeling, the SC was introduced in a capillary for the ESR measurement. Under these conditions the SC was considered to be in the fully hydrated state (the excess of water). The value obtained for the average hydration for this sample from gravimetric measurements was 58 ± 7% (w/w). After ESR measurements, the fully hydrated samples were recovered from the capillaries, dried in the desiccator, and divided in five parts, and then each one was placed in the desiccator in order to obtain different levels of water content (at equilibrium with 93, 81, 62, 46, and 0% of RH). After 3 days in desiccator, the samples were introduced into capillaries again for new measurements. These capillaries having a volume about twice that of the samples were immediately sealed in order to maintain a constant hydration during the experiment. The absence of changes in hydration level was ascertained by the temperature reversibility of the ESR signals.

ESR The measurements were performed on a Varian E-9 spectrometer equipped with the rectangular cavity. Temperature was controlled with a nitrogen stream system from Air Products and Chemicals Inc. (Allentown, PA). ESR spectra were obtained at X-band (9.150 GHz) with a microwave power of 20 mW, a modulation frequency of 100 KHz, and an amplitude of 2.5 G. The sweep time was 4 min, the magnetic field scan was 100 G, and the detector time constant was 0.064 s.

ESR Spectra Analysis Generally the fluidity of a membrane can be estimated from the order parameter S, which can be calculated according to Gaffney (1976) using an expression which includes the apparent parallel and perpendicular hyperfine splitting parameters of the spectrum $T'_{\parallel}$ and $T'_{\perp}$ **(Fig 2)**, and an empirical correction for the difference between the true and apparent polarity. Since the resolution of $2T'_{\perp}$ is very poor at low temperatures, we used the dependence of $2T'_{\parallel}$ to monitor temperature changes for 5-SASL and 12-SASL.

In the rapid motion regime like in the case of 16-SASL the resolution of $2T'_{\parallel}$ becomes insufficient for precise determination from the experimental spectra **(Fig 2c)**. However, the use of the rotational correlation time τ_c can be made for the analysis of the spectra (Simon, 1979):

$$\tau_c = K \cdot W_0[(h_0/h_{-1})^{1/2} - 1], \quad (1)$$

where $K = 6.5 \times 10^{-10}$ s · G^{-1}, and W_0 is the peak-to-peak linewidth of the central line ($M_I = 0$), h_0 and h_{-1} are the intensities of the central and high field lines, respectively **(Fig 2)**.

Water Flux in SC (WFSC) The experiment was performed according to Blank *et al* (1984). SC was mounted in a glass diffusion chamber, and 0.8 ml of the aqueous solution of K_2CO_3 was put in both the donor and receptor sides of the chamber in order to control the RH of the environment at 31°C. Only the vapor above the solutions, which had a RH dependence on K_2CO_3 concentration, contacted the SC. During the 3-day period, the SC came to equilibrium with the environment, and after that, 20 μl of tritiated water (HTO) was introduced into the solution on the donor side through the septum using a microsyringe. After 3 more days, 20-μl samples of donor and receptor solutions were counted in 3 ml of scintillation fluid (toluene 2.4 ml, methanol 0.48 ml, and Liquifluor 0.12 ml) using a Beckman (model LS 100) liquid scintillation counter. In the steady state the WFSC for HTO was calculated using the following expression:

$$J = \frac{R}{D} \cdot \frac{W}{A \cdot t}, \quad (2)$$

where J is the steady-state flux of HTO (mg · cm^{-2} · h^{-1}), R is counts per min (CPM) in receptor solution, D is CPM in donor solution, W is weight of solution at donor and receptor sides (800 mg), A is exposure area of SC (0.54 cm^2), and t is exposure time (hours).

We assumed that the receptor count is always very low as compared to donor count (~500,000 CPM) and the return flux of HTO from receptor to donor was negligible. We also assumed that the permeability constants of H_2O and HTO are identical.

Elasticity The curves of mechanical tension versus displacement of SC were measured with a Zuick Tensiometer (model 1445, Germany). The following parameters were obtained from the curves: the elastic modulus, the rupture tension, and the elongation of SC (respectively, EMSC, RTSC, ESC). The width of the SC strip was 14 mm, the length (in the direction of displacement) was 22 mm, and the velocity of displacement was 0.5 mm · min^{-1}. The water content was controlled in a desiccator, and the measurements were performed at ambient temperature (25 ± 3°C).

Electrical Resistance of SC (ERSC) The measurements were made with a Keithley Electrometer (model 617, U.S.A.) and a pair of platinum electrode with flat faces having an area of 3.8 cm^2. The SC taken from the desiccator was placed between the electrode faces, and the readings were taken 5 s after the contact.

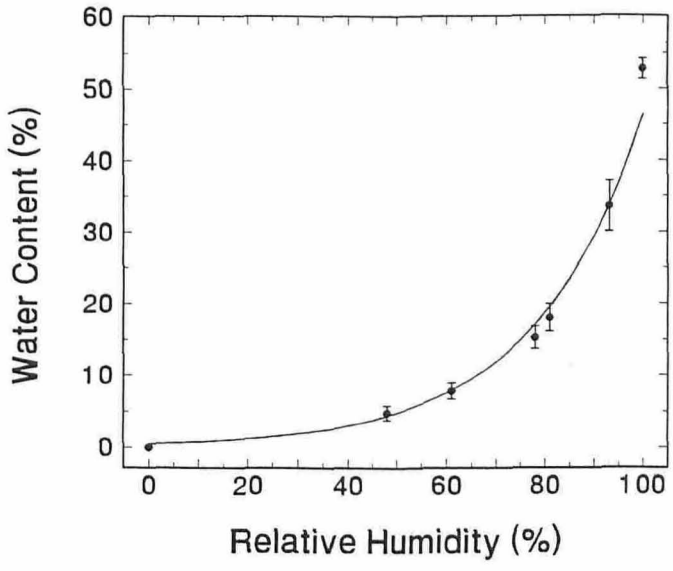

Figure 1. Water content (w/w in the wet tissue) in neonatal rat stratum corneum in equilibrium with different relative humidity levels of the environment at 31°C. *Error bar*, mean ± SD for n = 6.

RESULTS

WCSC **Figure 1** presents the effect of RH on the water binding capacity of neonatal rat SC in the equilibrium at 31°C. We assumed that the equilibrium WCSC at 0% RH is very small. Our data for neonatal rat are similar to those obtained by Spencer *et al* (1975) and Blank *et al* (1984) for human SC. The data can be fit (correlation coefficient: r = 0.98) to an exponential function:

$$\text{WCSC} = 0.447\exp(0.047 \times RH), \quad (3)$$

with WCSC expressed as w/w and RH in percentage. The exponential behavior of WCSC versus RH shows that the mechanism of water uptake by the SC can be understood as a water

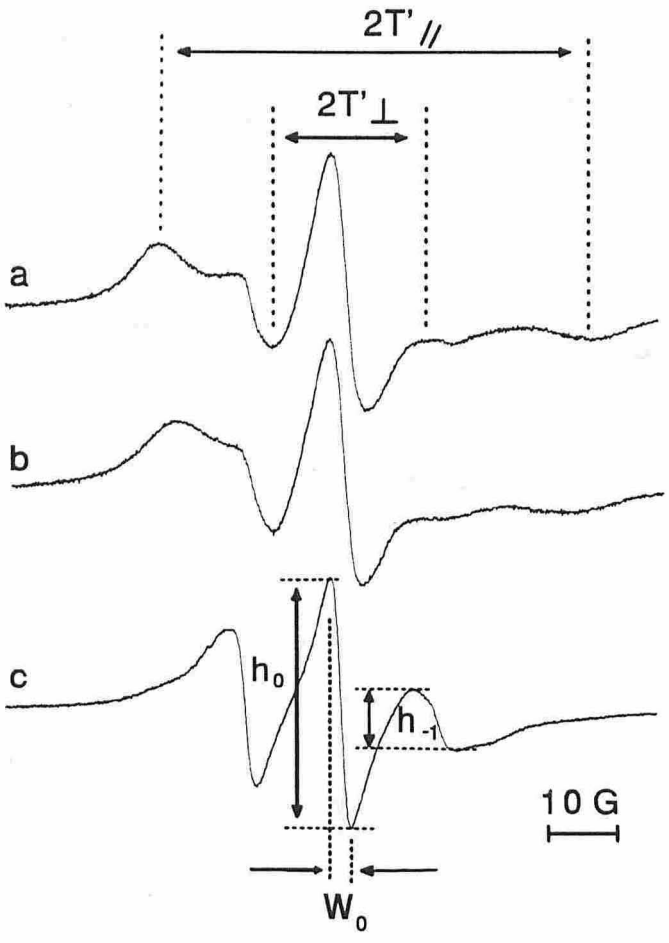

Figure 2. ESR spectra of spin labels 5-, 12-, and 16-SASL (*a*, *b*, *c*, respectively) in intercellular membranes of stratum corneum fully hydrated (phosphate-buffered saline, pH 7.4) at 37°C. The measured parameters are indicated.

cooperative effect. At low WCSC, the water is tightly bound and probably causes conformational changes of the protein keratin producing more binding sites with lower affinity and increasing the capacity to store water, even if it is loosely bound.

ESR The spectra at 37°C for 5-, 12-, and 16-SASL in SC are shown in **Fig 2**. ESR spectra are similar to the spectra observed in plasma membranes, and are characteristic for highly immobilized labels, as could be expected for the rigid SC membranes (Elias, 1977, 1981). This membrane rigidity is due mostly to its high cholesterol content (20–25% of total lipids) and the large amount of ceramides (40–50%) (Gray *et al*, 1982; Long *et al*, 1985) with mainly saturated long chains containing 22 or 26 carbon atoms (Elias, 1988). Nitroxide reduction was not observed for these spin labels (Alonso *et al*, 1995a) in contrast with our observations for the spin labels Tempo and Tempol (Alonso *et al*, 1995b) and for perdeuterated di-*t*-butyl nitroxide (Rehfeld *et al*, 1990). This indicates that the stearic acid spin labels are located almost exclusively in the SC membrane.

No ESR magnetic interaction among the spin labels was observed, thus showing that the spin labels were uniformly distributed among the membrane lipids of SC. Given about 14% of SC lipids (Gray *et al*, 1982), we can estimate the mean lipid:spin label molar ratio to be about 160; this is quite sufficient to avoid the dipolar interaction (Fung and Johnson, 1984).

At low temperature and/or WCSC, sometimes we failed to resolve the $2T'_{\parallel}$ parameter, and, therefore, to calculate the order parameter S. The parameters $2T'_{\parallel}$, $2T'_{\perp}$ and S are the static parameters associated to the orientational distribution of spin labels in the membrane, although they are related to the changes in spin label mobility. The $2T'_{\parallel}$ parameter generally decreases with membrane fluidity, and therefore can be used for its characterization. Another parameter, the rotational correlation time τ_c, is directly associated with the motional reorientation of the spin label and consequently with the probe mobility in the membrane. In the case of 16-SASL the parameters $2T'_{\parallel}$ and $2T'_{\perp}$ are not resolved in the spectra **(Fig 2)** and therefore the use of τ_c is more reliable.

In **Fig 3** the parameter $2T'_{\parallel}$ for 5-SASL and for 12-SASL and the parameter τ_c for 16-SASL are plotted as a function of WCSC for three temperatures (31°, 37°, and 45°C). The membrane fluidity increased with the hydration level of the SC. The effect is more pronounced for the 5-SASL where the nitroxide group is near the polar headgroups of the lipids, suggesting that, at the membrane/water interface, where water interacts strongly with the membrane, the changes in the probe motion are greater. At higher temperatures the effect for 5-SASL **(Fig 3*A*)**, almost did not change for 12-SASL **(Fig 3*B*)** and diminished in the τ_c measurements for 16-SASL **(Fig 3*C*)**.

Water Flux of SC (WFSC) **Figure 4** shows the steady state flux J of HTO through SC in equilibrium with different RHs of the environment, plotted as a function of RH or corresponding WCSC values (according to **Fig 1**). We included a theoretical point in **Fig 4*B*** postulating a zero flux at 0% RH. The first four experimental points (at 46, 62, 78, and 81% of RH) together with the theoretical point at 0% RH can be nicely fit to a linear function ($r = 0.99$), while the last two experimental points (at 93 and 100% of RH) are well above this straight line. According to Fick's law, under steady-state conditions

$$J = K_m \cdot D \cdot (\Delta c/\delta), \tag{4}$$

where K_m is the partition coefficient of water in SC given by the ratio of concentrations ($mg \cdot cm^{-3}$) of HTO in SC and in the solution, D is the diffusion coefficient, Δc is the difference of HTO concentration at donor and receptor sides, and δ is the membrane thickness. Under steady-state conditions, J is constant across the membrane at each RH value. In the isothermic and isovolumic diffusion chamber, Δc is proportional to RH, and

$$J = K \cdot RH, \tag{5}$$

where $K = K_m \cdot (D/\delta) \cdot (\Delta c/RH)$ or

$$K = Kp \cdot (\Delta c/RH) \tag{6}$$

is a positive constant and K_p is the permeability constant. Equations 5 and 6 show that the dependence of J vs RH is linear if K_p of SC is constant for all WCSC values. From the data presented in **Fig 4*B***, this seems to occur for RH up to 81%. Above this RH, which corresponds to 18% WCSC, an increase in the slope of the curve shows an increase in permeability, in agreement with the increase in fluidity at the C-5 position of the acyl chain in this range of water content **(Fig 3*A*)**. It is clear from Equation 6 that K_p can increase due to an increase either in K_m or D, because δ increases with RH (Blank *et al*, 1984). Blank *et al* also calculated both K_m and D for human SC and suggested that the increase in K_m or D with WCSC plays an important role in the mechanism that controls the transepidermal water loss.

Elasticity **Figure 5** shows the elastic modulus, rupture tension, and elongation of neonatal rat SC as a function of the WCSC. The EMSC and the RTSC showed a biphasic behavior. At hydration below ~33% (w/w) an approximately exponential decay of both is observed and, therefore, the semilogarithmic plots give a straight line in this region. At higher water contents the additional water behaved like a bulk liquid, affecting very slightly these parameters. The curve of ESC vs WCSC **(Fig 5*C*)** has a sigmoidal shape. At WCSC below ~18% (w/w) the ESC practically does not change undergoing a sharp increase between ~20 and 33% (w/w) of water content. Above ~33% of WCSC, the changes in ESC, similarly to EMSC and RTSC, are not significant.

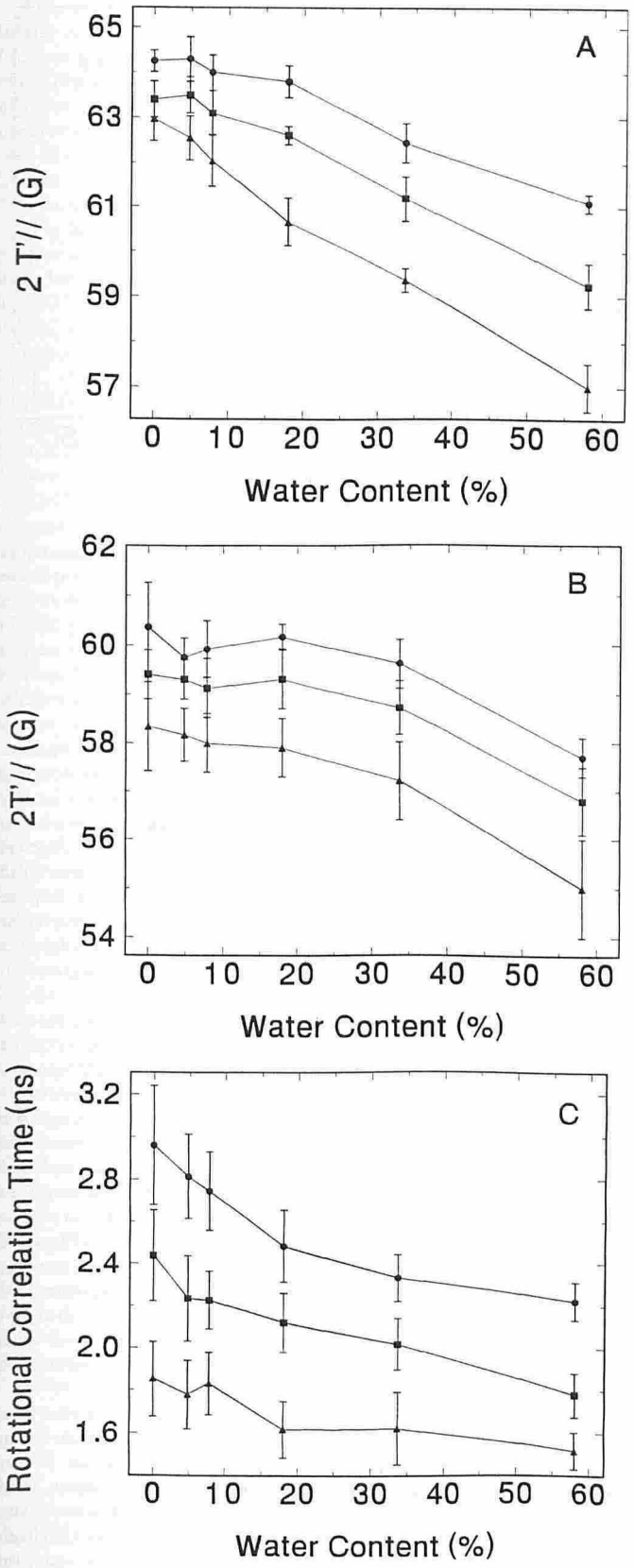

Figure 3. ESR parameter $2T'_{\parallel}$ for the spin labels 5-SASL (*A*) and 12-SASL (*B*) and rotational correlation time, τc, for 16-SASL (*C*) in intercellular membrane of neonatal rat stratum corneum at three different temperatures as a function of its water content. The measurement temperatures are: 31°C (*circles*), 37°C (*squares*) and 45°C (*triangles*). *Error bar*, mean ± SD for n = 3.

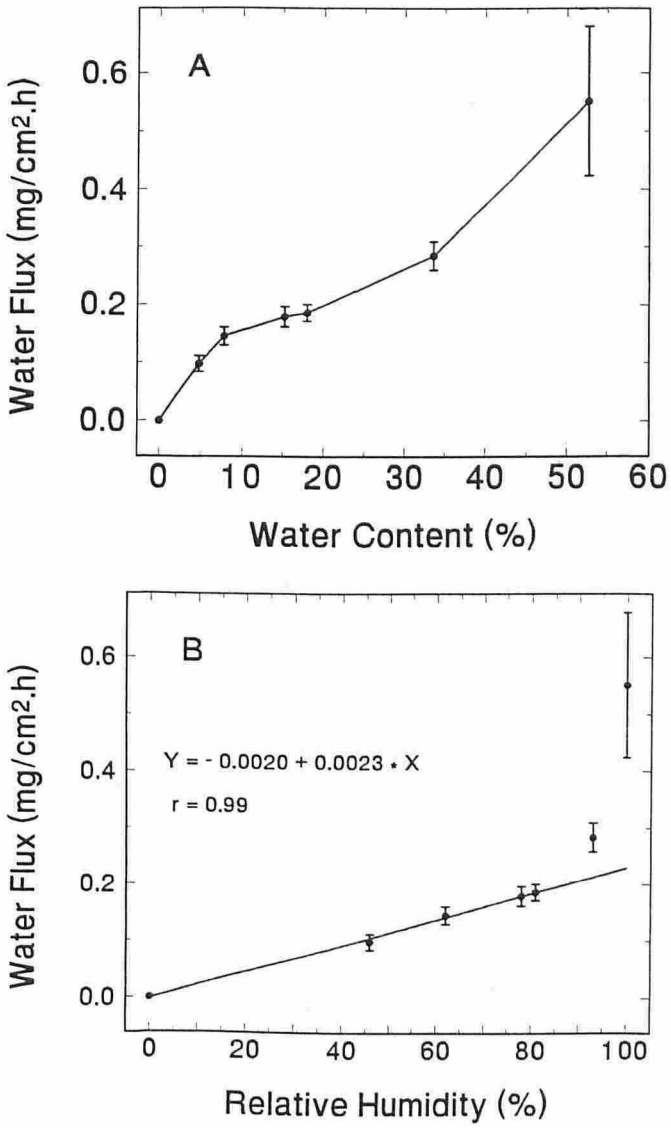

Figure 4. Steady-state water flux *J* in neonatal rat stratum corneum at 31°C as a function of (*A*) its water content (w/w in wet tissue), and (*B*) relative humidity (*RH*). The equation is the linear regression for the first five points. *Error bar*, mean ± SD for n = 6.

ERSC The ERSC in direction transversal to the membrane plane is plotted as a function of WCSC in **Fig 6**. Up to approximately 25% (w/w) of water content, ERSC showed an exponential fall with the increase of WCSC (r = 0.99), and above this hydration level, the reduction was less pronounced.

DISCUSSION

Hansen and Yellin (1972) have employed infrared and nuclear magnetic resonance (NMR) spectroscopy to investigate the mechanism of water uptake by human SC. The infrared results showed that water molecules exist in three different states, depending on the water content. Converting their data relative to weight of wet SC, one can characterize these states as follows: a) below ~9% (w/w), water is tightly bound to the polar sites of SC proteins (primary hydration); b) From ~9 up to ~28% (w/w), water is bound to the primary water by hydrogen bonds; and c) above ~33% (w/w), the water properties do not differ from those of bulk water. The NMR relaxation measurements revealed at least two time constants, suggesting lower water mobility at low water

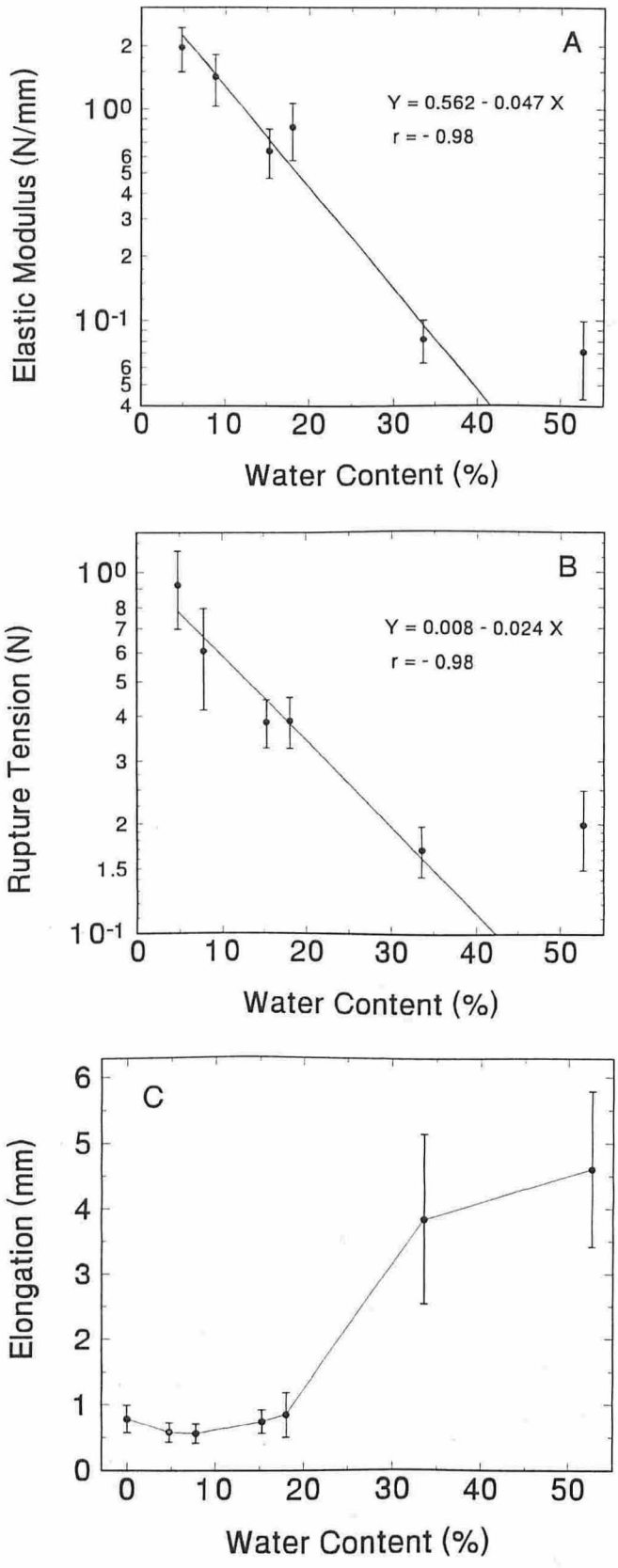

Figure 5. Elasticity parameters of neonatal rat stratum corneum as a function of its water content (w/w in wet tissue). The equations into *A* and *B* are linear regressions on the first five experimental points (logarithmic scale). *Error bar*, mean ± SD for n = 6.

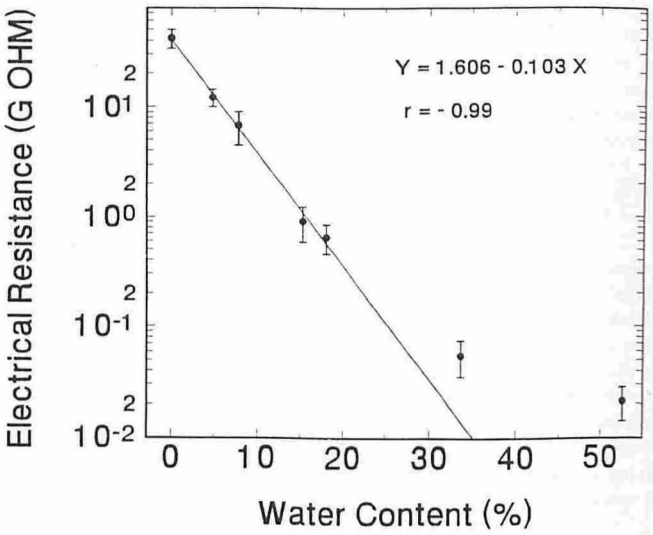

Figure 6. Electrical resistance in neonatal rat stratum corneum as a function of its water content (w/w in wet tissue). The equation is the linear regression for the first five experimental points (logarithmic scale). *Error bar*, mean ± SD for n = 6.

content and the mobility similar to that of bulk water above ~23% (w/w).

Fettyplace and Haydon (1980) reported that artificial as well as biological membranes show increasing permeability with increasing membrane fluidity. Hydration increases the water diffusion in SC (El-Shime and Princen, 1978; Blank *et al*, 1984) and has been considered as a very effective enhancer for drug permeation (Barry, 1987; Potts and Francoeur, 1991). Our results show that the membrane fluidity does increase with the water content in the neonatal rat SC. The increase in fluidity is larger in the layer near the polar headgroup (C-5 position), where water molecules form a small hydration shell that could enlarge the free space for segmental motion of the first carbons in the acyl chain.

It is interesting to note that the changes of $2T'_{\parallel}$ for both 5- and 12-SASL are more significant above 18% WCSC, while τ_c for 16-SASL, which depends essentially on the free interchain spaces, experiences major changes below 18% at all three temperatures **(Fig 3)**. An increase in the rotational motion of nitroxide at the C-16 position below 18% WCSC may be rationalized in terms of the hydration of the protein keratin resulting in the volume expansion of the corneocyte and widening of free interchain spaces until all water binding sites of the protein are occupied.

WFSC and τ_c are not in a relationship on would expect **(Figs 3*C* and 4*B*)**. In our case τ_c changes mainly up to 18% WCSC, exactly where K_p is constant, and only smaller variations were observed above this water content where K_p and WFSC increase sharply. This shows that the SC permeability is more closely associated with the fluidity of the intercellular membrane of the SC in the region near the polar headgroups.

Golden *et al* (1987) measured the activation energy for water flux in porcine SC and found a value of ~17 kcal/mol, which is in agreement with the values obtained for the diffusion of water through hydrocarbon domains measured in lipid bilayers and liposomes (Knutson *et al*, 1986; Golden *et al*, 1987). Because the results are similar, the authors suggest that the water flux through the SC is limited by diffusion through the ordered hydrocarbon domain of the intercellular lipids. Our work shows a direct correlation between water flux and membrane fluidity in SC. Thus, the transepidermal water loss may be controlled by membrane fluidity of the SC. Penetration through the region of the first carbon atoms of the acyl chains where the fluidity is lower should be the rate-limiting step for water transport, in agreement with our data.

The water loss *in vivo* for neonatal rat is similar to human skin being about 3.0 $g \cdot m^{-2} \cdot h^{-1}$ at an ambient RH of 50–60%. (Servomed evaporimeter, data not shown.) Based on the data *in vitro* **(Fig 4*A*)**, we can estimate the water content of the outer layers of neonatal rat SC *in vivo* to be ~33%. This value is considerably greater than the values observed *in vitro* at the same RH **(Fig 1)**. It can be explained by the contact of outer layers with the more hydrated innermost layers of the SC and by the continuous water flux across the SC *in vivo*.

The biomechanical properties of the SC determine the viscoelastic properties of the epidermis (Christensen *et al*, 1977). These properties have been assessed *in vivo* using special instrumentation (Christensen *et al*, 1977; Maes *et al*, 1983; Cooper *et al*, 1985) that measure objectively the SC contribution. This methodology shows that the skin hydration is important for the improvement of the elasticity at the skin surface level. Our results show that the elasticity parameters EMSC, RTSC, and ESC change mainly at low WCSC when the filling of water binding sites of the proteins occurs **(Figs 5*A* and 5*B*)**. Probably, these parameters are dependent only on the keratin properties in the SC. Above 33% WCSC alterations are insignificant, and below 18% WCSC the protein is insufficiently hydrated so that the SC looses its elongation capacity **(Fig 5*C*)**. Since there is a gradient of water concentration across the SC in the direction inside the body, the outer cell layers of SC have the lower water content and, therefore, they experience a stronger mechanical stress. This phenomenon could have a biological function in the mechanism of normal and abnormal skin desquamation. These outer cell layers also are the rate-limiting for the transepidermal water loss due to their lower water content.

Leveque and Rigal (1983) reviewed the impedance methods for measuring SC moisturization. As they pointed out, the water molecules are able to form a continuous network of hydrogen bonds, and the presence of an electrical field allows the proton to exchange between H_3O^+ and OH^- within the SC and, thus, generates the current. Among other mechanisms proposed to explain how water can change the electrical properties of the SC, this seems to be the more direct and important one. Within this conception, in the region of WCSC where the network of hydrogen bonds is being formed (below ~25%), the behavior of ERSC versus WCSC is an exponential decay, and above this WCSC the decay is slight.

The results of this study show that there exist two critical levels of WCSC: about 18% and 33%. Below 18% of WCSC, a mobility of deepest parts of hydrocarbon lipid chains increases along with the major changes in elastic and electric properties of SC membrane. Above 18% WCSC, the hydration of the polar region of SC membrane increases its fluidity, and the efficiency of water transport through the membrane builds up sharply. The mobilization of the middle part of hydrocarbon chains occurs at WCSC above 33%, when elastic and electric parameters become hydration-independent.

These studies show an application of the ESR technique and membrane spin probes as a fine methodology to analyze the fluidity behavior of intercellular lamellae of intact SC. This approach may be used to investigate drug-lipid interactions in the SC, as well as different cases of skin diseases and lesions.

This work was supported by Conselho Nacional de Desenvolvimento Científico e Tecnológico (CNPq) grant process 300908/92-0. We thank Prof. Dr. Carlos Rettori and Prof. Dr. Gaston Barberis for the support given to this work.

REFERENCES

Alonso A, Meirelles NC, Tabak M: Effect of hydration upon the fluidity of intercellular membranes of stratum corneum: an ESR study. *Biochim Biophys Acta* 1237:6–15, 1995a

Alonso A, Meirelles NC, Tabak M: Stratum corneum intercellular lipid as compared to erythrocyte ghosts: an ESR study of thermotropic behavior and nitroxide reduction. *Physiol Chem Phys Med NMR* 27:63–72, 1995b

Barry BW: Penetration enhancers. *Pharmacol Skin* 1:121–137, 1987

Blank IH, Moloney J, Emslie AG, Simon I, Apt C: The diffusion of water across the stratum corneum as a function of its water content. *J Invest Dermatol* 82:188–194, 1984

Christensen MS, Hargens CW, Nacht S, Gans EH: Viscoelastic properties of intact human skin instrumentations, hydration effects and contribution of the stratum corneum. *J Invest Dermatol* 69:282–286, 1977

Cooper ER, Missel PJ, Hannon DP, Albright GB: Mechanical properties of dry, normal, and glycerol-treated skin as measured by the gas-bearing electrodynamometer. *J Soc Cosmet Chem* 36:335–348, 1985

Elias PM: Epidermal lipids, membranes and keratinization. *Int J Dermatol* 20:1–19, 1981

Elias PM: Epidermal lipids, barrier function, and desquamation. *J Invest Dermatol* 80:44s-49s, 1983

Elias PM: Structure and funtion of the stratum corneum permeability barrier. *Drug Dev Res* 13:97–105, 1988

Elias PM, Friend DS: The permeability barrier in mammalian epidermis. *J Cell Biol* 65:180–191, 1975

Elias PM, Goerke J, Friend DS: Mammalian epidermal barrier layer lipids: composition and influence on structure. *J Invest Dermatol* 69, 535–546, 1977

El-Shime AF, Princen HM: Diffusion characteristics of water vapor in some keratins. *Colliod and Polymer Sci* 256:209–217, 1978

Fettyplace R, Haydon DA: The permeability of lipid membranes. *Physiol Rev* 60:510–550, 1980

Fung LWM, Johnson ME: Recent developments in spin label EPR methodology for biomembrane studies. In: Lee P (ed.). *Current topics in bionergetics*. Academic Press, New York, 1984, pp 107–157

Gaffney BJ: Practical considerations for the calculation of order parameters for fatty acid or phospholipid spin labels in membranes. In: Berliner LJ (ed.). *Spin labeling theory and applications*. Academic Press, New York, 1976, pp 567–571

Golden GM, McKie JE, Potts RO: Role of stratum corneum lipid fluidity in transdermal drug flux. *J Pharm Sci* 76:25–28, 1987

Gray GM, White RJ, Yardley HJ: Lipid composition of the superficial stratum corneum cells of the epidermis. *Br J Dermatol* 106:59–63, 1982

Hadgraft J, Walters KA, Guy RH: Epidermal lipids and topical drug delivery. *Sem Dermatol* 11:139–144, 1992

Hansen JR, Yelin W: NMR and infrared spectroscopic studies of stratum corneum hydration. In: Jellinek HHG (ed.). *Water structure and the water-polymer interface*. Plenum Publishing Co., New York, 1972, pp 19–28

Knutson K, Potts RO, Guzek DB, Golden GM, McKie JE, Lambert WJ, and Higuchi WI: Macro- and molecular physical-chemical considerations in understanding drug transport in the stratum corneum. In: *Advances in Drug Delivery Systems*. Anderson JM, Kim SW (eds.). Elsevier, Amsterdam, 1986, pp 67–87

Leveque JL, Rigal J: Impedance methods for studying skin moisturization. *J Soc Cosmet Chem* 34:419–428, 1983

Long SA, Wertz PW, Strauss JS, Downing DT: Human stratum corneum polar lipids and desquamation. *Arch Dermatol Res* 277:284–287, 1985

Maes D, Short J, Turek BA, Reinstein JA: *In vivo* measuring of skin softness using the gas bearing electrodynamometer. *Int J Cosmet Sci* 5:189–200 1983

Potts RO, Francoeur ML: The influence of stratum corneum morphology on water permeability. *J Invest Dermatol* 96:495–499, 1991

Rehfeld SJ, Plachy WZ, Hou SYE, Elias PM: Localization of lipid microdomains and thermal phenomena in murine stratum corneum and isolated membrane complexes: an electron spin resonance study. *J Invest Dermatol* 95:217–223, 1990

Serban GP, Henry SM, Cotty VF, Cohen GL, Riveley JA: Electrometric technique for the *in vivo* assessment of skin dryness and the effect of chronic treatment with a lotion on the water barrier function of dry skin. *J Soc Cosmet Chem* 34:383–393, 1983

Simon I: Differences in membrane unsaturated fatty acids and electron spin resonance in different types of myeloid leukemia cell. *Biochim Biophys Acta* 556:408–442, 1979

Spencer TS, Linamen CE, Akers WA, Jones HE: Temperature dependence of water content of stratum corneum. *Br J Dermatol* 93:159–164, 1975

Swartzendruber DC, Wertz PW, Kitko DJ, Madison KC, Downing DT: Molecular models of the intercellular lipid lamellae in mammalian stratum corneum. *J Invest Dermatol* 92:251–257, 1989

Swartzendruber DC, Wertz PW, Madison KC, Downing DT: Evidence that the corneocyte has a chemically bound lipid envelope. *J Invest Dermatol* 88:709–713, 1987

White SH, Mirejovsky D, King GI: Structure of lamellar lipid domains and corneocyte envelopes of murine stratum corneum. An X-ray diffraction study. *Biochemistry* 27:3725–3732, 1988